Available online at www.sciencedirect.com
ScienceDirect
Journal of Nuclear Materials 360 (2007) 49–57
journal of nuclear materials
www.elsevier.com/locate/jnucmat

Investigation of electrorefining of metallic alloy fuel onto solid Al cathodes

L. Cassayre, R. Malmbeck *, P. Masset, J. Rebizant, J. Serp, P. Soucek, J.-P. Glatz

European Commission, Joint Research Centre, Institute for Transuranium Elements, P.O. 2340, 76125 Karlsruhe, Germany

Abstract

This work concerned the electrorefining of UZr and UPuZr alloys on a solid aluminium cathode, in the LiCl–KCl eutectic melt containing U^{3+}, Pu^{3+}, Np^{3+}, Zr^{2+} or Zr^{4+}, Am^{3+}, Nd^{3+}, Y^{3+}, Ce^{3+} and Gd^{3+} chlorides. During constant current electrolyses, the use of a cathodic cut-off potential (−1.25 V versus Ag/AgCl) allowed to selectively deposit actinides (mainly U), while lanthanides remained in the salt. The aim was to determine the maximal load achievable on a single aluminium electrode. The total exchange charge was 4300 C, which represents the deposition of 3.72 g of actinides in 4.17 g Al, yielding a composition of 44.6 wt% An in Al. It was shown that the melting of the cathode contributed to increase the total amount of actinides deposited on the aluminium.

1. Introduction

One important criterion for future innovative reactor systems is sustainability including minimisation of waste output and its radiotoxicity. In this sense, the radiotoxic character of actinides (Np, Pu, Am, Cm) has a key impact and their recycling is mandatory [1,2]. For homogenous recycling of all actinides, pyrochemical separation schemes involving molten salt or molten metal media seem today the most suitable. Thermodynamic calculations have shown that aluminium could be the most promising metallic solvent to support the grouped recovery of actinides (An) and an efficient separation from lanthanides (Ln) [3,4]. In molten fluoride salts, the technique of reductive extraction is under development, with a separation process based on the different distribution of An and Ln between the salt and metallic Al phase [5].

In molten chloride media, the An–Ln separation is being developed using electrochemical techniques. It has already been shown that a selective separation of actinides can be achieved by electrolysis onto solid Al cathodes in the LiCl–KCl eutectic, with the formation of stable An–Al surface alloys [6]. In previous experiments, constant current electrolyses have been carried out on Al rod electrodes ($S \sim 4\ cm^2$) to characterise the alloys formed by electrodeposition of U^{3+} dissolved in the melt [7]. In these tests, the anodic reaction consisted in the electrochemical dissolution of uranium, by the use of a metallic U–Zr alloy as anode. The current density was gradually increased and adjusted until a stable cathodic potential was

* Corresponding author. Tel.: +49 7247 951 376; fax: +49 7247 95199611.
E-mail address: rikard.malmbeck@cec.eu.int (R. Malmbeck).

0022-3115/$ - see front matter © 2006 Elsevier B.V. All rights reserved.
doi:10.1016/j.jnucmat.2006.08.013

reached (~ -1.10 V versus Ag/AgCl), corresponding to the potential of formation of a uranium–aluminium alloy. SEM–EDX mapping revealed the presence of the UAl_4 alloy as expected by the U–Al binary phase diagram at the experimental temperature (450 °C) [8].

In such an electrolytic process, the rate of the alloy formation depends on the diffusion of the involved elements in and through the solid alloy phase. Thus with increasing thickness of the alloy, further deposition of An as An–Al alloy becomes more and more difficult. If the deposition rate of An is too high, a depletion of Al occurs at the surface and the actinides will deposit as pure metals, at potentials shifted towards more negative values. This must be avoided, since for an efficient grouped separation of actinides from lanthanides a potential more anodic than -1.25 V versus Ag/AgCl is required. The applied current has to be lowered as soon as the cathodic potential becomes too negative. However, a point is finally reached when it is no more possible to maintain the cathodic potential positive enough to ensure the separation of An from Ln. This limits the amount of An which can be recovered onto Al.

In order to further develop this pyrochemical process for separation of An onto solid Al cathodes, this study has focussed on evaluating the maximum amount of actinides that can be collected on a single Al electrode. This paper also discusses the limitation induced by low concentration of actinides when a cut-off potential is used.

2. Experimental

The experiments, storage and handling of chemicals were carried out in a glovebox under purified Ar atmosphere (less than 5 ppm of water and oxygen). An alumina double compartment crucible was used as a container (Fig. 1). The two compartments were filled with 10.93 g of Bi pellets and 4.62 g of Al pellets respectively. In order to provide an electrical lead to the Al cathode, the temperature was raised to 665 °C (the melting point of aluminium is 661 °C) and a Ta wire was inserted in the molten Al pool. As the temperature was reduced to 450 °C, the Al solidified and the Ta wire was attached. By solidifying, the Al cathode formed an irregular metal ball having an undefined surface area. Considering a spherical shape, the area was estimated to be 3–5 cm^2. The chloride salt was finally added in the crucible. It contained U^{3+}, Pu^{3+}, Np^{3+}, Zr^{2+} or Zr^{4+}, Am^{3+}, Nd^{3+}, Y^{3+}, Ce^{3+} and Gd^{3+}, dissolved in 40 g of LiCl–KCl eutectic (Aldrich 99.99%).

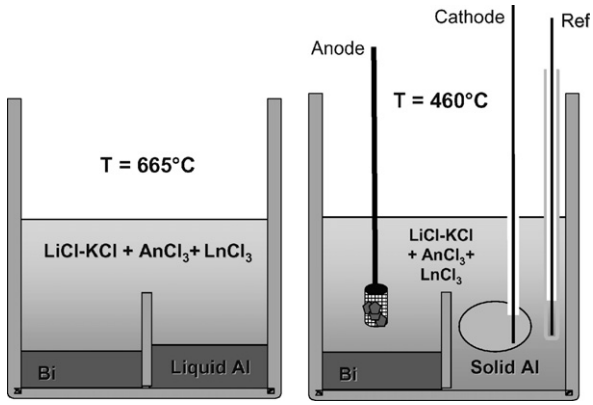

Fig. 1. Experimental set-up used in the electrorefining experiments.

The melt was first investigated by cyclic voltammetry at 450 °C, using either tungsten wire or aluminium wire (1 mm in diameter) as working electrode, the aluminium ball as counter electrode and an Ag/LiCl–KCl–AgCl (1 wt%) reference electrode. All potential values mentioned in this text refer to the Ag/AgCl (1 wt%) equilibrium potential.

Then, constant current electrolyses were carried out, the cathodic reaction being the selective reduction of An. The anodic reaction consisted in the dissolution of UZr (80/20 wt%) or UPuZr (71/19/10 wt%) alloys loaded in a Ta basket placed above the Bi pool. During the electrolyses, the anodic, cathodic and cell potentials were monitored versus the Ag/AgCl reference electrode.

Salt samples were regularly collected with a glass tube and the concentration of An–Ln was analysed by ICP-MS and XRF [9].

3. Results and discussion

3.1. Cyclic voltammetry

The melt was first investigated by cyclic voltammetry on a W working electrode. A cyclic voltammogram of the initial salt phase is presented in Fig. 2. Characteristic reduction peaks of trivalent An and Ln are observed during the sweep from anodic to cathodic potentials. The first cathodic wave is attributed to the reduction of uranium (U^{3+} to U^0) at -1.50 V. This is followed by the reduction of Np^{3+} to Np^0 at -1.69 V (not clearly visible), the

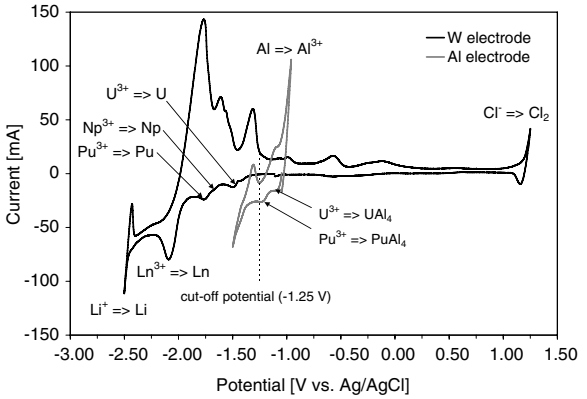

Fig. 2. Cyclic voltammogram on W and Al wires. Reference electrode: Ag/AgCl-1 wt%, $v = 100$ mV/s, $T = 450$ °C. Salt composition in wt%: U-0.29, Np-0.12, Pu-0.28, Am-0.06, Zr < 0.07 and Ln-1.0.

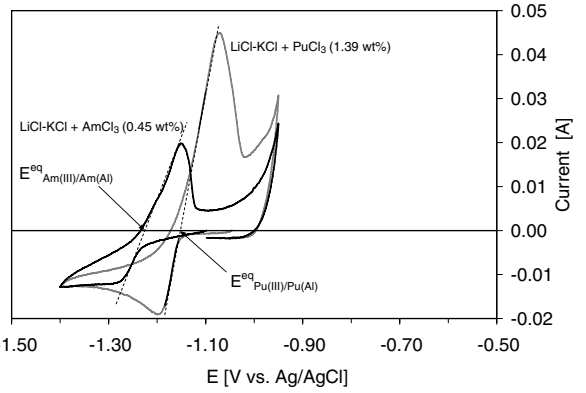

Fig. 3. Cyclic voltammograms on Al wire in LiCl–KCl + 1.39 wt% $PuCl_3$ and in LiCl–KCl + 0.45 wt% $AmCl_3$. Reference electrode: Ag/AgCl-1 wt%, $v = 100$ mV/s, $T = 450$ °C.

deposition of Pu at −1.77 V and the reduction of Ln^{3+} to Ln^0 at around −2.00 V [10]. Due to the low concentration of Am^{3+} (0.06 wt%), its reduction is not detected by cyclic voltammetry, but occurs at a potential in between the Pu and the Ln reduction potentials [11]. The cathodic limit of the solvent is reached at −2.50 V, where Li^+ is reduced to Li metal.

The W working electrode was then replaced by an Al wire in order to investigate the best conditions to perform the selective electrolysis of the An onto the Al cathode. A cyclic voltammogram is plotted in Fig. 2. As the metals alloy with Al, their reduction potentials shift to more positive values compared to the reduction potentials on the inert W cathode [6]: U^{3+} is reduced to UAl_4 at −1.05 V and Pu^{3+} to $PuAl_4$ at −1.17 V. The Am and Np concentrations are too low to detect clear reduction signals on the Al electrode. Lanthanides start reducing at potentials more negative than −1.35 V.

For a better evaluation of the An–Ln reduction potentials on the aluminium electrode, LiCl–KCl melts containing only one compound (U, Pu, Np, Am or Nd) were prepared. Fig. 3 presents two voltammograms obtained in two LiCl–KCl melts containing $PuCl_3$ (1.39 wt%) and $AmCl_3$ (0.45 wt%), respectively. These voltammograms allowed a graphic determination of the equilibrium potentials $E^{eq}_{M(III)/M(Al)}$ of each compound, as shown in Fig. 3.

The measured equilibrium potentials $E^{eq}_{M(III)/M(Al)}$ can be expressed with the activity coefficients in the salt phase and in the metal phase. For instance, in the case of the U(III)/U(0) system, the equilibrium potential of the UAl_4 alloy is

$$E^{eq}_{U(III)/U(Al)} = E^{0}_{U(III)/U(0)} + \frac{RT}{3F}\ln\frac{a_{UCl_3}}{a_{U(Al)}}, \quad (1)$$

where $E^{0}_{U(III)/U(0)}$ is the standard potential of the U(III)/U(0) redox couple, a_{UCl_3} and $a_{U(Al)}$ are the activity of UCl_3 in the salt and of uranium in Al, respectively.

The apparent standard potential, $E^{*0}_{U(III)/U(0)}$ of the U(III)/U(0) redox couple is

$$E^{*0}_{U(III)/U(0)} = E^{0}_{U(III)/\ U(0)} + \frac{RT}{3F}\ln\gamma_{UCl_3}, \quad (2)$$

where $\gamma_{UCl_3} = \frac{a_{UCl_3}}{X_{UCl_3}}$ is the activity coefficient of UCl_3 and X_{UCl_3} is the molar fraction of UCl_3 in the salt.

Combining Eqs. (1) and (2), $E^{eq}_{U(III)/U(Al)}$ can be expressed as

$$E^{eq}_{U(III)/U(Al)} = E^{*0}_{U(III)/U(0)} + \frac{RT}{3F}\ln X_{UCl_3} - \frac{RT}{3F}\ln a_{U(Al)}. \quad (3)$$

Then, by introducing the apparent standard potential of reduction of UCl_3 onto Al, which is defined as:

$$E^{*0}_{U(III)/U(Al)} = E^{*0}_{U(III)/U(0)} - \frac{RT}{3F}\ln a_{U(Al)} \quad (4)$$

and by combining Eqs. (3) and (4), the equilibrium potential is finally expressed as

$$E^{eq}_{U(III)/U(Al)} = E^{*0}_{U(III)/U(Al)} + \frac{RT}{3F}\ln X_{UCl_3}. \quad (5)$$

Using Eq. (5) and the equilibrium potentials measured on the voltammograms, the apparent standard potentials on Al were determined. Results are listed in Table 1, along with additional data

Table 1
Derived apparent standard potentials of An and Ln on Al

Element	$E^{*0}_{M(III)/M(Al)}$ (V) versus Ag/AgCl (1 wt%)
U	−0.89, −0.92[a]
Np	−1.02
Pu	−1.03, −1.07[a]
Am	−1.08
Nd	−1.20, −1.28[b]
La	−1.28[b]
Y	−1.33[b]
Ce	−1.24[b]
Pr	−1.25[b]

[a] Calculated potential according to tabulated thermochemical data (see Eq. (9)).
[b] Experimental data from [11].

concerning lanthanides from Bermejo [12], measured in molten LiCl–KCl by electrochemical techniques.

Another way of evaluating the apparent standard potential is to calculate it from tabulated thermochemical data, using the energy of formation of $AnAl_4$ alloys. In this case, the only data available concern UAl_4 and $PuAl_4$ alloys [13]. For uranium, the corresponding electrochemical cell is

$$4Al_{(s)} + UCl_{3(dissolved)} + 3Ag_{(s)} = UAl_{4(s)} + 3AgCl_{(dissolved)}. \quad (6)$$

The equilibrium potential $E^{eq}_{U(III)/U(Al)}$ can be expressed as

$$E^{eq}_{U(III)/U(Al)} - E^{eq}_{Ag(I)/Ag} = E^{0}_{U(III)/UAl_4} - E^{0}_{Ag(I)/AgCl} + \frac{RT}{3F}\ln\frac{a_{UCl_3}}{a^3_{AgCl}}, \quad (7)$$

where $E^{eq}_{Ag(I)/Ag} = 0$ V since it is the reference potential, $E^{0}_{U(III)/UAl4} - E^{0}_{Ag(I)/AgCl} = -\frac{\Delta_r G^0}{3F}$, $\Delta_r G^0$ being the standard Gibbs energy of Eq. (6),

$$a_{UCl_3} = \gamma_{UCl_3} X_{UCl_3},$$

a_{AgCl} is equal to the molar fraction X_{AgCl}, assuming unity activity coefficient for AgCl [14].

From Eq. (7) comes:

$$E^{eq}_{U(III)/U(Al)} = \left[-\frac{\Delta_r G^0}{3F} - \frac{RT}{F}\ln X_{AgCl} + \frac{RT}{3F}\ln\gamma_{UCl_3}\right] + \frac{RT}{3F}\ln X_{UCl_3}. \quad (8)$$

Comparison of Eqs. (5) and (8) allows expressing the standard apparent potential as

$$E^{*0}_{U(III)/U(Al)} = -\frac{\Delta_r G^0}{3F} - \frac{RT}{F}\ln X_{AgCl} + \frac{RT}{3F}\ln\gamma_{UCl_3}, \quad (9)$$

where $-\frac{\Delta_r G^0}{3F} = -1.15$ V according to data from Chiotti [13] and Barin [15], $\gamma_{UCl_3} = 2.0\times10^{-3}$ according to data from [16], $X_{AgCl} = 3.25\times10^{-3}$ (1 wt%). At 450 °C, the calculated value of the apparent standard potential according to Eq. (9) is −0.92 V, which is close to the value derived from measurement (−0.89 V) as shown in Table 1. For Pu(III)/Pu(Al), calculation was also consistent with experimental value, since the calculated apparent standard potential is equal to −1.12 V (with an activity coefficient of 3.5×10^{-3} [10] and $-\frac{\Delta_r G^0}{3F} = -1.32$ V [13,15]).

The data shown in Table 1 clearly confirm that a selective extraction of An is feasible, provided that the potential of the Al electrode is not too negative.

3.2. Electrolysis experiments

Before starting electrorefining, the concentration of uranium was increased by adding UZr into the Bi pool and oxidising it by the addition of $BiCl_3$ in the salt phase, as described in [16]. The uranium concentration was thereby increased to 1 wt%, allowing the use of higher currents during the electrolysis. The resulting composition of the melt is presented in Table 2.

An were collected in the Al cathode by constant current electrorefining. Each run was controlled by maintaining a cathodic potential suitable for separation of An from Ln, i.e., more positive than −1.25 V (see dashed vertical line in Fig. 2). As soon as the

Table 2
Initial composition of the electrolyte

Element	Initial concentration (wt%)
Y	0.04
Ce	0.05
Nd	0.28
Gd	0.61
Zr	0.007
U	1.05
Np	0.12
Pu	0.28
Am	0.06

cathodic potential dropped below −1.25 V, the current density was reduced in order to slow down the reaction and ensure a selective An deposition.

During the night the cathode was lifted up and maintained 1 cm above the bath, at roughly 400 °C. On some occasions the temperature of the bath was raised to 700 °C and the Al cathode was melted in order to homogenise the deposit and create a fresh surface. In total more than 70 electrolyses were performed by applying currents in a 10–50 mA range, and the total charge passed was around 4300 C.

3.2.1. Potential evolution during electrorefining

Fig. 4 shows the evolution of the potential of the Al electrode as well as the applied current during the complete experiment.

In the first electrolysis, at 30 mA, a total charge of 250 C was passed before the cathodic current reached the limit of −1.25 V. The second electrolysis at 20 mA involved a total charge of 210 C before interruption. The cathode was then lifted up and kept at 400 °C over the bath for several days before the experiment continued. In the next electrolyses a higher current could be used and a total charge of 220 C was passed at currents between 30 and 40 mA. This was followed by a few electrolyses passing roughly 550 C with currents decreasing from 35 to 15 mA. The next set of experiments performed 48 h later in a series of electrolyses involving some 340 C of which 220 C was passed at a current of 20 mA.

Although the applied current had to be gradually decreased with increasing total charge passed, it appeared that maintaining the cathode above the melt between each run had a beneficial effect, due to the inter-diffusion of An and Al.

After a total charge of 1500 C had been passed (corresponding to approximately 1.25 g of An), the applied currents had to be kept at a maximum of 20 mA, with frequent stops imposed by the cut-off potential. The cathode was often maintained above the bath to allow the diffusion of the deposited An into the bulk of the aluminium. Between 2500 and 3100 C, the effect of Al saturation became more and more evident. As shown in Fig. 4, the frequency of the stops increased, and thus the length of each run decreased accordingly.

After 3100 C were exchanged, 2.59 g of actinides had been deposited in 4.62 g of Al, according to Faraday's law. This corresponds to an An loading of the electrode of 35.9 wt%. At this point, the Al cathode was heated to 700 °C in order to homogenise its composition and create a fresh Al-rich surface for further alloying (see * in Fig. 4). According to the U–Al binary phase diagram presented in Fig. 5, a complete homogenisation of the alloy is not possible at this temperature. However, pure unused Al in the centre of the cathode probably melted, thus improving the life time of the cathode for further electrorefining.

After this process, it was again possible to electrolyse at 30 mA for longer runs. Finally, between 4000 C and 4300 C, the Al cathode was melted several times without significant positive effects. At this point the experiment was stopped.

In total a charge of 4300 C was electrolysed at an average current of 25 mA, corresponding to the

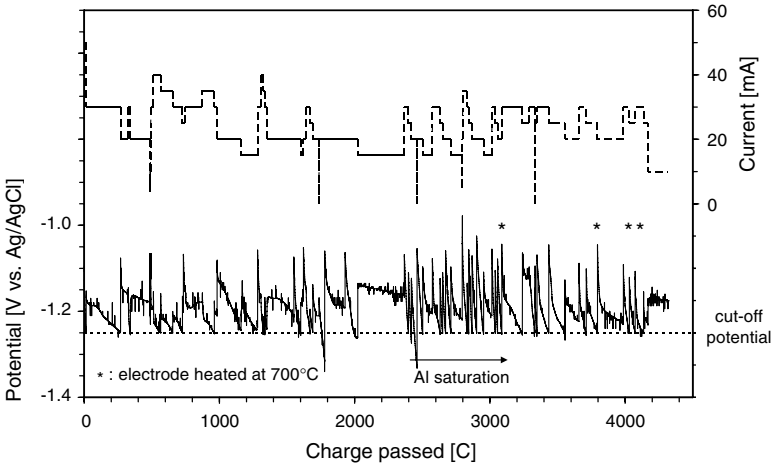

Fig. 4. Cathodic potential and applied current during the complete experiment.

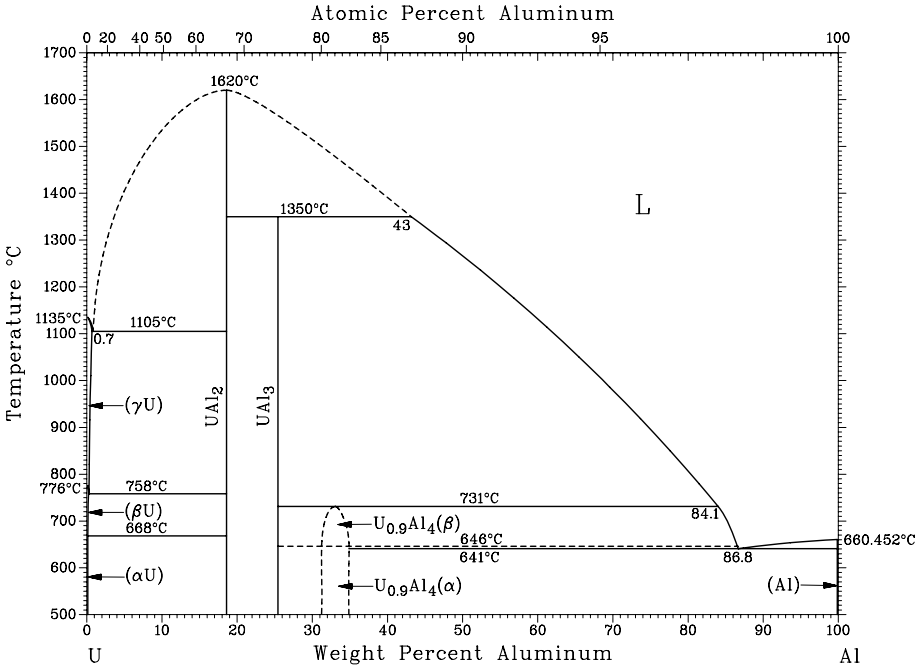

Fig. 5. U–Al phase diagram [8]. Copyright© 1996 by ASM International.

reduction of 3.72 g of actinides in 4.17 g of Al. This yields a total loading of 44.6 wt% An in Al. The recovered Al cathode (after washing in methanol to remove adhering salt) is shown in Fig. 6. On top, the Ta lead and a small piece of the Al_2O_3 tube can be seen. The white areas show small amounts of remaining salt.

During the experiment, the potential of the anode basket was around −1.30 V, which corresponds to the anodic dissolution of U^{3+} from the UZr alloy (80–20 wt%). After 1600 C the anode potential suddenly increased and the electrolysis was stopped. According to the weight and composition of the UZr alloy, at this point the anode was depleted in U and the positive jump in anodic potential indicated the start of Zr dissolution (above −1.0 V) [17]. The anode was then replaced by the UPuZr alloy. After 2800 C the same rise in anodic potential effect was observed, and the anode was replaced after roughly 3200 C. A third basket containing UZr alloy was used as anode for the end of the experiment.

3.2.2. Salt analysis

The evolution of An–Ln concentrations in the salt is shown in Fig. 7. The corresponding anode basket composition is also reported on this plot.

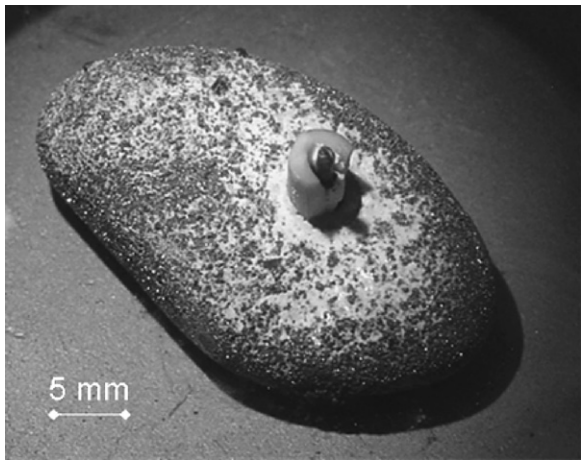

Fig. 6. Al cathode, washed in methanol after the experiment.

3.3. Ln

During the whole experiment the concentration of lanthanides (Gd, Nd, Ce and Y) remained stable, which means that the cathodic potential was positive enough to avoid their reduction.

3.4. U

During electrorefining using the UZr anode, U was anodically dissolved but also reduced at the

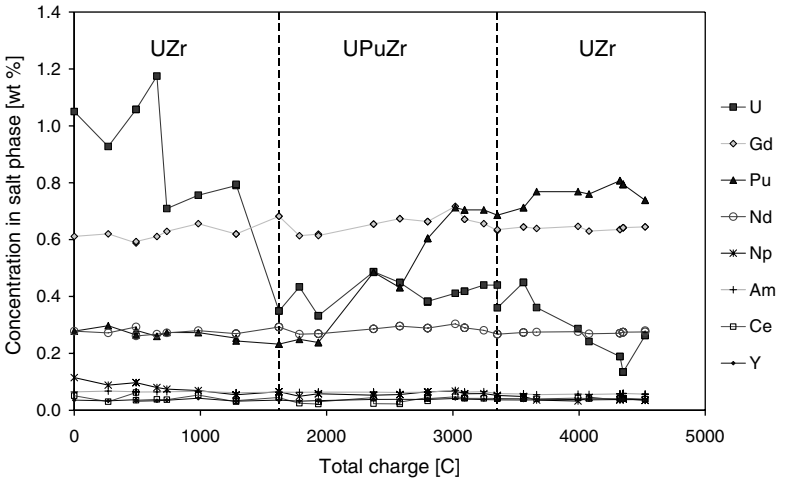

Fig. 7. Salt concentration versus total charge.

cathode, which means that the concentration of uranium should remain fairly constant. However, during passage of the first 1500 C charge, the uranium concentration decreased from approximately 1 wt% to 0.4 wt%. This represents a uranium loss in the bath of about 250 mg compared to the 1.23 g of actinides oxidised and collected on the cathode. One possible reaction that could account for this is the chemical reductive extraction of U^{3+} onto Al, because the potential of U–Al alloy formation is close (less than 50 mV) to the Al open-circuit potential.

At the end of the experiment, as the anode material was changed back to UZr, a slight decrease in U concentration was also observed. During these last runs the Al cathode was heated several times at 700 °C, which might have enhanced the chemical reaction between Al and U^{3+}.

3.5. Pu

During the first part of the electrorefining (involving the UZr anode), the amount of Pu in the melt should decrease, since Pu is co-reduced at the cathode and not balanced by the anodic reaction. A small decrease in Pu concentration (from 0.28 wt% to 0.23 wt%) is actually observed in Fig. 7.

When the anode was replaced by an UPuZr alloy, the anodic dissolution led to an increase of the concentration of Pu^{3+}. Indeed, the concentration of Pu increased from 0.3 wt% up to 0.7 wt% between 2000 and 3000 C, which corresponds approximately to the amount of Pu released by congruent dissolution of the anode. At the end of the experiment, as the anode material was changed back to UZr, the concentration of Pu remained roughly stable.

These measurements show that during the electrorefining, U^{3+} is mainly reduced compared to Pu^{3+}. The deposition of U is indeed enhanced by the fact that the reduction potential of U^{3+} is more positive (~150 mV) than the reduction potential of Pu^{3+}, and that during a large part of the electrorefining, the cathodic potential is more positive than −1.15 V.

3.6. Am–Np

As shown in Fig. 8, some Np was co-reduced onto the Al cathode. Indeed, the Np concentration decreased from 0.12 wt% down to about 0.04 wt%. Am concentration remained stable during the complete experiment at 0.06 wt%.

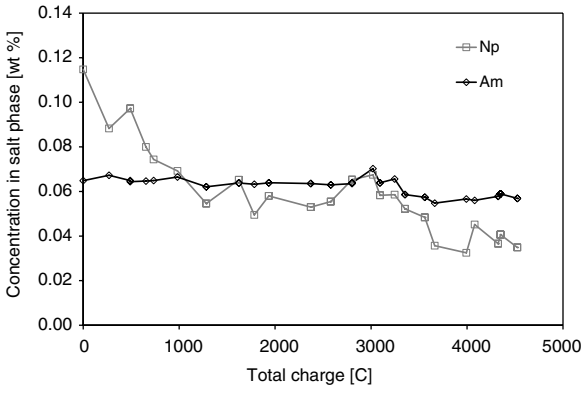

Fig. 8. Salt concentration of Np and Am.

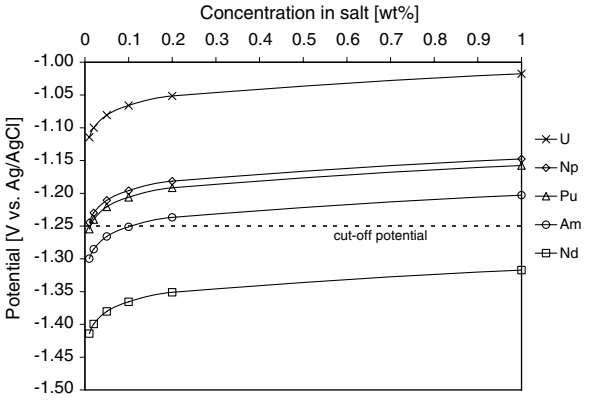

Fig. 9. Calculation of the influence of concentration on the reduction potential of U, Np, Pu, Am and Nd on an aluminium electrode in LiCl–KCl at 450 °C.

According to the Nernst equation, the reduction potential of a dissolved cation in the melt will shift towards a more negative value when its concentration decreases. If, as in this experiment, a cathodic cut-off potential is used, the recovery of Pu, Np and Am will be possible as long as their concentrations are high enough to allow their reduction onto the cathode. The required concentration is lower for Np and Pu than for Am as their reduction potentials onto Al are more positive (see Table 1). This is in agreement with the data presented in Figs. 7 and 8, since Np and Pu concentrations slightly decrease while Am concentration remains stable. It is also in good agreement with the calculated evolution of the reduction potentials on the aluminium cathode, plotted in Fig. 9. These potentials were calculated according to Eq. (5), using standard potentials from Table 1. According to Fig. 9, a slightly more negative cut-off potential (~ -1.30 V) should be used to extract more Am from the melt. In this case, previous experiments have shown that Ln would then be slightly more co-reduced [18].

4. Conclusions

The maximum An loading of a solid Al cathode has been investigated in constant current electrorefining experiments in which the cathodic potential was maintained at a suitable level for separation of An from Ln, i.e., more positive than −1.25 V versus Ag/AgCl. The anodic reaction was the dissolution of UZr or UPuZr alloy and the cathodic reaction was the reduction of An onto Al. With increased charged passed, i.e. with the build up of a surface layer of An–Al alloy, the applied current was gradually reduced in order to stay above the cathodic potential limit.

It was shown that keeping the cathode several days above the molten salt at elevated temperatures in between runs had a beneficial effect since higher currents could be used. This is due to the inter diffusion of the elements through the bulk of the cathode. In addition, melting of the cathode caused homogenisation of its composition and created a new Al-rich surface for further alloying, allowing further loading of the cathode.

Near the end of the experiment the cathode was melted several times but without significant positive effects on the current possible to use. At this stage approximately 4300 C had been exchanged, representing the reduction of 3.72 g of actinides in 4.17 g Al. This yields a composition of 44.6 wt% An in Al, which can be compared to the maximal loading of 68 wt% considering $AnAl_4$ alloys.

Salt analysis confirmed that the use of a cathodic cut-off potential (−1.25 V versus Ag/AgCl) allows to selectively deposit actinides (mainly U) and leave lanthanides in the salt. However Am was probably not deposited because its deposition potential at the used concentration (0.06 wt%) was below the cut-off potential. This effect will be an important issue when aiming at the complete removal of minor actinides (mostly Am, Cm) dissolved in the salt.

Acknowledgements

The authors wish to thank C. Scheppler for ICP measurements, B. Lynch for XRF measurements and M. Iizuka for his help with the data acquisition system. Part of this study was carried out with CEC financial support under the Sixth Framework Program under Management and Disposal of Radioactive Waste, Contract FP6-508854 (EUROPART).

References

[1] Actinide and Fission Product Partitioning and Transmutation – Status and Assessment report, OECD-NEA, 1999.
[2] Accelerator Driven Systems (ADS) and Fast Reactors (FR) in Advanced Nuclear Fuel Cycles – A Comparative study, OECD/NEA, 2002.
[3] V.A. Lebedev, Selectivity of liquid metal electrodes in molten halides (title translated), ISBN 5-229-00962-4, 1993 (in Russian).

[4] O. Conocar, N. Douyere, J.-P. Glatz, J. Lacquement, R. Malmbeck, J. Serp, Nucl. Sci. Eng. 153 (2006) 253.
[5] O. Conocar, N. Douyere, J. Lacquement, J. Nucl. Mater. 344 (1–3) (2005) 136.
[6] J. Serp, M. Allibert, A. Le Terrier, R. Malmbeck, M. Ougier, J. Rebizant, J.-P. Glatz, J. Electrochem. Soc. 152 (2005) C167.
[7] J. Serp, R. Malmbeck, E. Yakub, J.-P. Glatz, in: Proc. of GLOBAL 2003, New Orleans, 2003.
[8] T.B. Massalski, H. Okamoto, P.R. Subramanian, L. Kacprzak, Binary Alloy Phase Diagrams, second ed., ASM International, Ohio, 1990.
[9] S. Abousahl, P. van Belle, H. Eberle, H. Ottmar, B. Lynch, P. Vallet, K. Mayer, M. Ougier, Radiochim. Acta 93 (2005) 147.
[10] P. Masset, R.J.M. Konings, R. Malmbeck, J. Serp, J.-P. Glatz, J. Nucl. Mater. 344 (2005) 173.
[11] J. Serp, P. Chamelot, S. Fourcaudot, R.J.M. Konings, R. Malmbeck, C. Pernel, J.C. Poignet, J. Rebizant, J.-P. Glatz, Electrochim. Acta 51 (19) (2006) 4024.
[12] R. Bermejo, PhD thesis, Facultad de ciencas, Valladolid, 2003 (in Spanish).
[13] P. Chiotti, V.V. Akhachinskij, I. Ansara, M.H. Rand, The Chemical thermodynamics of actinide elements and compounds. Part 5. The actinide binary alloys, IAEA, Vienna, 1981.
[14] J.J. Roy, L.F. Grantham, D.L. Grimmett, S.P. Fusselman, C.L. Krueger, T.S. Storvick, T. Inoue, Y. Sakamura, N. Takahashi, J. Electrochem. Soc. 143 (8) (1996) 2487.
[15] I. Barin, O. Knacke, O. Kubashewski, Thermochemical Properties of Inorganic Substances, Springer-Verlag, Berlin, 1991.
[16] P. Masset, P.D.W. Bottomley, R.J.M. Konings, R. Malmbeck, A. Rodrigues, J. Serp, J.-P. Glatz, J. Electrochem. Soc. 152 (6) (2005) A1109.
[17] M. Iizuka, K. Kinoshita, T. Koyama, J. Phys. Chem. Solids 66 (2005) 427.
[18] J. Serp, R. Malmbeck, C. Scheppler, J.-P. Glatz, in: Proc. of ATALANTE 2004, Nîmes, 2004.